PERGAMON

International Journal of Solids and Structures 40 (2003) 1907–1921

INTERNATIONAL JOURNAL OF SOLIDS and STRUCTURES

www.elsevier.com/locate/ijsolstr

A unified periodical boundary conditions for representative volume elements of composites and applications

Zihui Xia *, Yunfa Zhang, Fernand Ellyin

Department of Mechanical Engineering, University of Alberta, Edmonton, Alta., Canada T6G 2G8

Received 29 April 2002; received in revised form 29 November 2002

Abstract

An explicit unified form of boundary conditions for a periodic representative volume element (RVE) is presented which satisfies the periodicity conditions, and is suitable for any combination of multiaxial loads. Starting from a simple 2-D example, we demonstrate that the "homogeneous boundary conditions" are not only over-constrained but they may also violate the boundary traction periodicity conditions. Subsequently, the proposed method is applied to: (a) the simultaneous prediction of nine elastic constants of a unidirectional laminate by applying multiaxial loads to a cubic unit cell model; (b) the prediction of in-plane elastic moduli for $[\pm\theta]_n$ angle-ply laminates. To facilitate the analysis, a meso/micro rhombohedral RVE model has been developed for the $[\pm\theta]_n$ angle-ply laminates. The results obtained are in good agreement with the available theoretical and experimental results.

Keywords: Fiber-reinforced composites; Micromechanical modeling; Unified periodical boundary conditions; Angle-ply laminate; Multiaxial loading

1. Introduction

Composite materials are becoming an essential part of present engineered materials because they offer advantages such as higher specific stiffness and strength, better fatigue strength and improved corrosion-resistance compared to conventional materials. They are used in various applications ranging from aerospace structures to sports equipment, electronic packaging, medical tools, and civil engineering structures. Consequently, prediction of the mechanical properties of the composites has been an active research area for several decades. Except for the experimental studies, either micro- or macromechanical methods are used to obtain the overall properties of composites.

Micromechanical method provides overall behavior of the composites from known properties of their constituents (fiber and matrix) through an analysis of a periodic representative volume element (RVE) or a unit-cell model (Aboudi, 1991; Nemat-Nasser and Hori, 1993). In the macromechanical approach, on the

* Corresponding author. Tel.: +1-780-492-3870; fax: +1-780-492-2200.
E-mail address: zihui.xia@ualberta.ca (Z. Xia).

0020-7683/03/$ - see front matter © 2003 Elsevier Science Ltd. All rights reserved.
doi:10.1016/S0020-7683(03)00024-6

other hand, the heterogeneous structure of the composite is replaced by a homogeneous medium with anisotropic properties. The advantage of the micromechanical approach is not only the global properties of the composites but also various mechanisms such as damage initiation and propagation, can be studied through the analysis (Xia et al., 2000; Ellyin et al., 2002).

There are several micromechanical methods used for the analysis and prediction of the overall behavior of composite materials. In particular, upper and lower bounds for elastic moduli have been derived using energy variational principles, and closed-form analytical expressions have been obtained (Hashin and Shtrikman, 1963; Hashin and Rosen, 1964). Based on an energy balance approach with the aid of elasticity theory, Whitney and Riley (1966) obtained closed-form analytical expressions for a composite's elastic moduli. Unfortunately, the generalization of this method to viscoelastic, elastoplastic and nonlinear composites is very difficult. Aboudi (1991) has developed a unified micromechanical theory based on the study of interacting periodic cells, and it was used to predict the overall behavior of composite materials both for elastic and inelastic constituents. In his work, homogeneous boundary conditions were applied to the RVE or unit cell models. In fact, this is only valid for those cases in which normal tractions are applied on the boundaries. For a shear loading case, many researchers, e.g., Needleman and Tvergaard (1993), Sun and Vaidya (1996), Suquet (1987), among others, have indicated that the 'plane-remains-plane' boundary conditions are over-constrained boundary conditions. In the current paper we shall further demonstrate that they are not only over-constrained boundary conditions but may also violate the stress/strain periodicity conditions.

The above micromechanical models can be regarded as mechanical or engineering models. A mathematical counterpart to such engineering methods appeared in the 1970s under the general heading of the 'asymptotic homogenization theory'. The fundamentals of this theory can be found, e.g. in Suquet (1987), Benssousan et al. (1978), Sanchez-Palencia (1980), and Bakhvalov and Panasenko (1984), among others. Asymptotic homogenization theory has explicitly used periodic boundary conditions in modeling of linear and nonlinear composite materials. These results have clearly shown that characteristic modes of deformation do not result in plane boundaries after deformation (Suquet, 1987). Guedes and Kikuchi (1991) discussed the application of finite element method (FEM) to composite problems. Recent applications of homogenization theory for various aspects of composite analysis are given, for instance, in Raghavan et al. (2001) and Moorthy and Ghosh (1998).

Hori and Nemat-Nasser (1999) presented a universal inequalities which indicate that the predicted effective elastic modulus can vary depending on the applied conditions on the boundary ∂V of a unit cell, and the homogeneous displacement and homogeneous traction boundary conditions will give the upper and lower bounds of the effective modulus. Hollister and Kikuchi (1992) have given a very good comparison of the homogenization theory and the mechanical methods (it is called average field theory in Hori and Nemat-Nasser (1999)), concluding that the homogenization theory, which uses the periodic boundary conditions, yields more accurate results. It is shown that the homogenization theory and mechanical methods can be related to each other and a more applicable hybrid theory was established (Hollister and Kikuchi, 1992).

FEM has been extensively used in the literature to analyze a periodic unit cell, to determine the mechanical properties and damage mechanisms of composites (Adams and Crane, 1984; Aboudi, 1990; Allen and Boyd, 1993; Bonora et al., 1994; Pindera and Aboudi, 1998). In most cases, the applications are limited to the unidirectional laminates. A few investigators have also applied the micromechanical analysis to the cross-ply laminates (laminates contain only 0° and 90° laminae), for which the thermal residual stresses, crack initiation and propagation, viscoplastic or viscoelastic behaviors have been studied (Xia et al., 2000; Ellyin et al., 2002; Bigelow, 1993; Chen et al., 2001).

In the present paper the FEM micromechanical analysis method is applied to unidirectional and angle-ply laminates subject to *multiaxial loading conditions*. For the latter laminates, special meso/micro *rhombohedral* RVE models have been developed. Based on general periodicity conditions stated by Suquet (1987),

an explicit form of boundary conditions suitable for FEM analyses of parallelepiped RVE models subjected to multiaxial loads is presented. Starting from a simple 2-D example, the results of the present method and those obtained by applying homogeneous boundary conditions are compared. Subsequently, the FEM analyses are conducted for two composite RVE models: (1) a unidirectional laminate to predict simultaneously all nine elastic constants by applying multiaxial loads; (2) a thick $[\pm\theta]_n$ angle-ply laminate to predict simultaneously the four in-plane elastic moduli by applying biaxial loads. The predicted properties are compared with available theoretical or experimental results and are found to be in very good agreement. Although the illustrative analyses presented in the current paper are limited to the elastic range, the basic relations proposed in this paper are independent of the properties of the constituents of the composite.

2. Representative volume elements for unidirectional and angle-ply laminates

The micromechanical model is set up based on the periodic RVE technique. For the continuous fiber reinforced composites, it is assumed that fibers are uniformly distributed in the matrix and have the same radii. Therefore, each unidirectional layer could be represented by a unit cube with a single fiber having the same fiber volume fraction as the ply, see Fig. 1. Instead of the square layout of fibers reflected by this RVE model, the square-diagonal or hexagonal RVE models have also been used (Li, 1999).

Fig. 2 indicates the manner in which a RVE is developed for a thick angle-ply $[\pm\theta]_n$ laminate. From the periodicity of the fiber array, we can cut a rhombohedral RVE consisting of two layers, each with a single

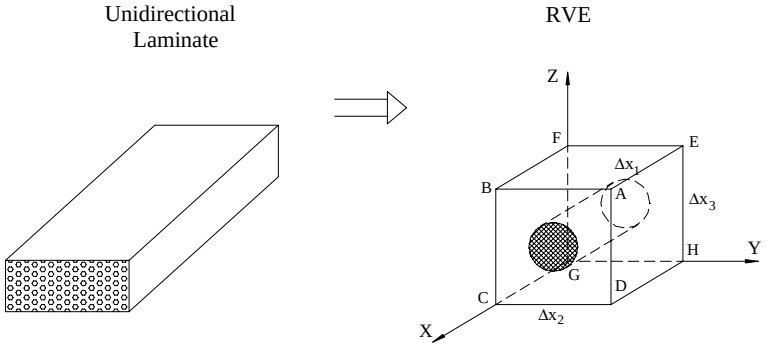

Fig. 1. A representative volume element for a unidirectional laminate.

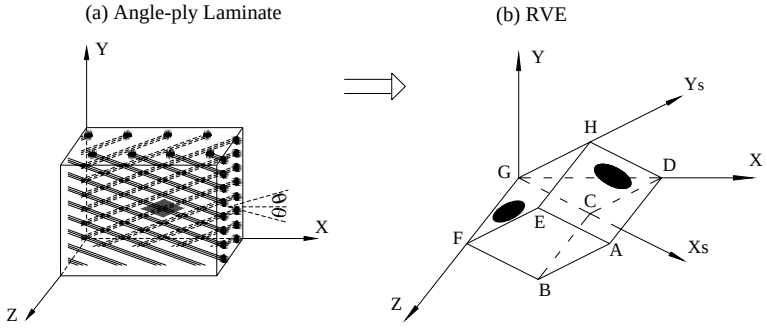

Fig. 2. A representative volume element for an $[\pm\theta]$ angle-ply laminate.

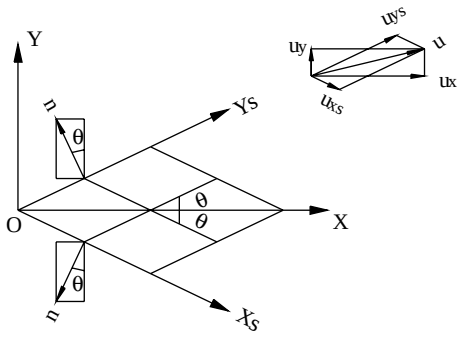

Fig. 3. The two coordinate systems.

fiber in the direction $+\theta$ and $-\theta$, respectively. The angle-ply laminate can thus be seen as a periodical array of this unit cell.

It should be noted that in Fig. 2, the angle θ is measured from X axis (if measured from the Y axis, it will be $90^\circ - \theta$), therefore this model can also be seen as a RVE for the $[\pm(90-\theta)]_n$ laminates. For example, the RVEs for the $[\pm 30]_n$ laminates and the $[\pm 60]_n$ laminates are the same.

To facilitate the analysis, a skew coordinate system as shown in Fig. 3, is introduced. We denote this skew coordinate system as O–$X_sY_sZ_s$, with the same origin as that of the orthogonal coordinate system O–XYZ, and the axes X_s, Y_s are parallel to the fiber directions (direction of $\pm\theta$). In this system, the coordinates and the displacement components are designated as (x_s, y_s, z_s), and (u_{xs}, u_{ys}, u_{zs}), respectively. From Fig. 3, we can obtain the transformation between the two coordinate systems as follows:

$$\begin{Bmatrix} x_s \\ y_s \\ z_s \end{Bmatrix} = \frac{1}{\sin 2\theta} \begin{bmatrix} \sin\theta & -\cos\theta & 0 \\ \sin\theta & \cos\theta & 0 \\ 0 & 0 & \sin 2\theta \end{bmatrix} \begin{Bmatrix} x \\ y \\ z \end{Bmatrix} \tag{1}$$

$$\begin{Bmatrix} u_{xs} \\ u_{ys} \\ u_{zs} \end{Bmatrix} = \frac{1}{\sin 2\theta} \begin{bmatrix} \sin\theta & -\cos\theta & 0 \\ \sin\theta & \cos\theta & 0 \\ 0 & 0 & \sin 2\theta \end{bmatrix} \begin{Bmatrix} u_x \\ u_y \\ u_z \end{Bmatrix} \tag{2}$$

Referring to Fig. 2(b), we assume that S is the area of side surface (ABCD), ℓ is the length of the side AB, h is the height of the RVE (AD), S_1 is the area of the cross section (AEFB), the volume of the RVE is V, the fiber volume fraction is V_f and R is the radius of the fiber. The following relations between these geometric parameters can be obtained:

$$\begin{aligned} h &= 2\ell \sin 2\theta \\ S_1 &= \ell^2 \sin 2\theta \\ S &= 2\ell^2 \sin 2\theta \\ V &= 2\ell^3 \sin^2 2\theta \\ R &= \ell \sin 2\theta \sqrt{\frac{V_f}{\pi}} \end{aligned} \tag{3}$$

3. Unified periodic boundary conditions for parallelepipedal RVE under multiaxial loading

Composite materials can be envisaged as a periodical array of the RVEs. Therefore, the periodic boundary conditions must be applied to the RVE models. This implies that each RVE in the composite has the same deformation mode and there is no separation or overlap between the neighboring RVEs. As stated by Suquet (1987), these periodicity conditions on the boundary ∂V is

$$u_i = \bar{\varepsilon}_{ik} x_k + u_i^*, \quad u_i^* \text{ periodic} \tag{4}$$

In the above $\bar{\varepsilon}_{ik}$ are the average strains, u_i^* is the periodic part of the displacement components on the boundary surfaces and it is generally unknown and is dependent on the applied global loads. A more explicit form of periodic boundary conditions, suitable for parallelepiped RVE models can be derived from the above general expression.

For a cubic RVE as shown in Fig. 1, the displacements on a pair of opposite boundary surfaces (with their normals along the X_j axis) are

$$u_i^{j+} = \bar{\varepsilon}_{ik} x_k^{j+} + u_i^* \tag{5}$$

$$u_i^{j-} = \bar{\varepsilon}_{ik} x_k^{j-} + u_i^* \tag{6}$$

where index "$j+$" means along the positive X_j direction and "$j-$" means along the negative X_j direction. The difference between the above two equations is

$$u_i^{j+} - u_i^{j-} = \bar{\varepsilon}_{ik}(x_k^{j+} - x_k^{j-}) = \bar{\varepsilon}_{ik} \Delta x_k^j. \tag{7}$$

For any parallelepiped RVE models Δx_k^j is constant, therefore the following unified periodic boundary conditions is obtained:

$$u_i^{j+}(x,y,z) - u_i^{j-}(x,y,z) = c_i^j \quad (i,j = 1,2,3) \tag{8}$$

The constants, c_1^1, c_2^2 and c_3^3, represent the average stretch or contraction of the RVE model due to the action of the three normal traction components, whereas the other three pairs of constants, $c_1^2 = c_2^1$, $c_1^3 = c_3^1$ and $c_2^3 = c_3^2$, correspond to the shear deformations due to the three shear traction components. This form of boundary conditions meets the requirement of displacement periodicity and continuity. It can be seen from Eq. (8) that although the difference of the displacements for the corresponding points on the two opposite boundary surfaces are specified, the individual displacement component is still a function of the coordinates, i.e. a plane does not necessarily remain a plane after the deformation. Also since Eq. (8) does not contain the periodic part of the displacement, which is unknown, it becomes easier to adopt this form in a finite element procedure, instead of applying (4) directly as the boundary conditions.

It is assumed that the average mechanical properties of a RVE are equal to the average properties of the particular composite laminate. The average stresses and strains in a RVE are defined by

$$\bar{\varepsilon}_{ij} = \frac{1}{V} \int_V \varepsilon_{ij} \, \mathrm{d}V \tag{9}$$

$$\bar{\sigma}_{ij} = \frac{1}{V} \int_V \sigma_{ij} \, \mathrm{d}V \tag{10}$$

where V is the volume of the periodic representative volume element.

The strain energies predicted by the different boundary conditions must satisfy the following inequality if the average strain $\bar{\varepsilon}_{ij}$ for each case is assumed to be the same (Suquet, 1987; Hori and Nemat-Nasser, 1999; Hollister and Kikuchi, 1992):

$$U^{\Sigma} \leqslant U^{P} \leqslant U^{E} \tag{11}$$

where U^{Σ}, U^{P}, U^{E} are the strain energy predicted by homogeneous traction boundary conditions, periodic boundary conditions, and homogeneous displacement boundary conditions, respectively. It is clear that the homogeneous displacement boundary conditions overestimate the effective moduli whereas the homogeneous traction boundary conditions underestimate the effective moduli. It should also be pointed out that the application of the homogeneous displacement boundary conditions generally would not guarantee to produce a periodic boundary traction. Similarly, the application of the homogeneous traction boundary conditions would not guarantee the displacement periodicity at the boundaries.

The calculation of average strain and stress can be simplified by using Gauss's theorem. The average strain in the RVE can be expressed as an integration around the boundary surfaces (Aboudi, 1991; Sun and Vaidya, 1996; Suquet, 1987)

$$\overline{\varepsilon}_{ij} = \frac{1}{V}\int_{V} \varepsilon_{ij}\,\mathrm{d}V = \frac{1}{2V}\int_{S} (u_i n_j + u_j n_i)\,\mathrm{d}S \tag{12}$$

Since all the boundary surfaces in Fig. 1 are perpendicular to one of the coordinate axis, the unit normal vector **n** has only one non-zero component on these surfaces with a value of unity. Therefore, using the symbols defined in Eq. (8), the above integration can be reduced to

$$\overline{\varepsilon}_{ij} = \frac{1}{2V}\left[\int_{S_j} (u_i^{j+} - u_i^{j-}) n_j\,\mathrm{d}S + \int_{S_i} (u_j^{i+} - u_j^{j-}) n_i\,\mathrm{d}S\right] = \frac{1}{2V}(c_i^j S_j + c_j^i S_i) = \frac{c_i^j \Delta x_i \Delta x_k + c_j^i \Delta x_j \Delta x_k}{2\Delta x_i \Delta x_j \Delta x_k}$$

Therefore,

$$\overline{\varepsilon}_{ij} = \frac{1}{2}\frac{c_i^j \Delta x_i + c_j^i \Delta x_j}{\Delta x_i \Delta x_j} \tag{13}$$

Note that the suffixes i and j in the above expressions are not dummy ones.

Likewise, by using the Gauss theorem and equilibrium equation $\sigma_{ij,j} = 0$, the average stress can be expressed as (Aboudi, 1991; Suquet, 1987)

$$\overline{\sigma}_{ij} = \frac{1}{V}\int_{S} \sigma_{ik} x_j n_k\,\mathrm{d}S \tag{14}$$

If one assumed that the stress distributions at the boundaries must also satisfy the periodicity condition, then at the two corresponding points on the two opposite planes (with same in-plane coordinates) must have the same normal and shear stresses. By a similar procedure as in the derivation of (13), Eq. (14) reduced to

$$\overline{\sigma}_{ij} = \frac{1}{V}\int_{S} \sigma_{ik} x_j n_k\,\mathrm{d}S = \frac{1}{V}\left(\int_{S_m^+} \sigma_{im}^+ x_j^+\,\mathrm{d}S - \int_{S_m^-} \sigma_{im}^- x_j^-\,\mathrm{d}S\right) = \frac{1}{V}\int_{S_m^+} \sigma_{im}^+ (x_j^+ - x_j^-)\,\mathrm{d}S$$

In the above the suffix m is a dummy suffix. However, when $m \neq j$, the coordinates $x_j^+ = x_j^-$ and when $m = j$, $x_j^+ - x_j^- = \Delta x_j$, therefore,

$$\overline{\sigma}_{ij} = \frac{\Delta x_j}{V}\int_{S_j} \sigma_{ij}\,\mathrm{d}S = \frac{P_{ij}}{S_j} \quad \text{(no summation over } j\text{)} \tag{15}$$

The above equation indicates that the average stresses can be simply obtained from the resultant tractions on the boundary surfaces by dividing them by the areas of the corresponding boundary surfaces.

For angle-ply laminates, the unified boundary conditions, Eq. (8) should be written in the skew coordinate system, O–$X_sY_sZ_s$, i.e.

$$u_{is}^{j+}(x_s, y_s, z_s) - u_{is}^{j-}(x_s, y_s, z_s) = c_i^j \tag{16}$$

In the above equation, all indices have the same meaning as in Eq. (8) except that they are now defined in the skew coordinate system.

If only in-plane loads are considered ($c_1^3 = c_3^1 = c_2^3 = c_3^2 = 0$) and by using the relation between the displacement components in the skew coordinate system and in the orthogonal *O–XYZ* coordinates, Eqs. (1) and (2), the displacement boundary conditions in the *O–XYZ* coordinates can be written as (note that the coordinates are expressed in the skew coordinate system in the following equations for clarity):

On planes ABCD ($x_s = \Delta x_s$) and EFGH ($x_s = 0$):

$$\begin{aligned}
&[u_x(\Delta x_s, y_s, z_s) - u_x(0, y_s, z_s)]\sin\theta - [u_y(\Delta x_s, y_s, z_s) - u_y(0, y_s, z_s)]\cos\theta = c_1^1 \sin 2\theta \\
&[u_y(\Delta x_s, y_s, z_s) - u_y(0, y_s, z_s)]\cos\theta + [u_x(\Delta x_s, y_s, z_s) - u_x(0, y_s, z_s)]\sin\theta = c_1^2 \sin 2\theta \\
&u_z(\Delta x_s, y_s, z_s) = u_z(0, y_s, z_s)
\end{aligned} \tag{17}$$

On planes ADHE ($y_s = \Delta y_s$) and BCGF ($y_s = 0$):

$$\begin{aligned}
&[u_x(x_s, \Delta y_s, z_s) - u_x(x_s, 0, z_s)]\sin\theta - [u_y(x_s, \Delta y_s, z_s) - u_y(x_s, 0, z_s)]\cos\theta = c_1^2 \sin 2\theta \\
&[u_y(x_s, \Delta y_s, z_s) - u_y(x_s, 0, z_s)]\cos\theta + [u_x(x_s, \Delta y_s, z_s) - u_x(x_s, 0, z_s)]\sin\theta = c_2^2 \sin 2\theta \\
&u_z(x_s, \Delta y_s, z_s) = u_z(x_s, 0, z_s)
\end{aligned} \tag{18}$$

On planes BAEF ($z_s = \Delta z_s$) and CDHG ($z_s = 0$):

$$\begin{aligned}
&[u_x(x_s, y_s, \Delta z_s) - u_x(x_s, y_s, 0)]\sin\theta - [u_y(x_s, y_s, \Delta z_s) - u_y(x_s, y_s, 0)]\cos\theta = 0 \\
&[u_y(x_s, y_s, \Delta z_s) - u_y(x_s, y_s, 0)]\cos\theta + [u_x(x_s, y_s, \Delta z_s) - u_x(x_s, y_s, 0)]\cos\theta = 0 \\
&u_z(x_s, y_s, 0) = 0 \\
&u_z(x_s, y_s, \Delta z_s) = c_3^3 = \text{const.}
\end{aligned} \tag{19}$$

Note that for the in-plane loading case, the constant c_3^3 is not required to be specified. Its value will be obtained through the FEM analysis. To eliminate the rigid body motion, the displacement components, u_x, u_y of the center point of the RVE are assumed to be zero.

To apply Eqs. (17)–(19) in the FEM analysis, the mesh in opposite boundary surfaces should be same. For each pair of displacement component at the two corresponding nodes with identical in-plane coordinates on the two boundary surfaces a constraint equation is imposed. Although a large number of the constraint equations needs to be applied, it is usually easy to produce all those equations by using certain automatic schemes embedded in a FEM package.

Based on definitions of the average strain and stress, Eqs. (9) and (10), using the similar procedures as in the derivations of Eqs. (13) and (15), and noting the geometric description of the RVE given by Eqs. (3), a relation between the average strains and the constants c_i^j, and the average stresses and resultant tractions on the boundary surfaces are found as follows:

$$\begin{aligned}
\bar{\varepsilon}_x &= \frac{1}{2l}(c_1^1 + 2c_1^2 + c_2^2) \\
\bar{\varepsilon}_y &= \frac{1}{2l}(c_1^1 - 2c_1^2 + c_2^2) \\
\bar{\varepsilon}_{xy} &= \frac{1}{l\sin 2\theta}(c_2^2 - c_1^1) \\
\bar{\varepsilon}_z &= \frac{c_3^3}{h}
\end{aligned} \tag{20}$$

$$\begin{aligned}\overline{\sigma}_x &= \frac{P_x^{AB} + P_x^{AE}}{2S\sin\theta}\\ \overline{\sigma}_y &= \frac{P_y^{AE} - P_y^{AB}}{2S\cos\theta}\\ \overline{\sigma}_{xy} &= \frac{P_x^{AE} - P_x^{AB}}{2S\cos\theta} = \frac{P_y^{AB} + P_y^{AE}}{2S\sin\theta}\end{aligned} \tag{21}$$

In Eqs. (21) P_x and P_y are the resultant tractions on the boundary surface which can be obtained directly from the FEA solutions.

4. Application examples

4.1. A 2-D illustrative example

To verify the unified boundary conditions, Eqs. (8), and the difference with the "homogeneous boundary conditions" (or plan-remains-plane boundary conditions), a 2-dimensional RVE model is considered. The model consists of a fiber reinforcement and matrix, with a volume fraction of 50%, Fig. 4. The elastic moduli and Poisson's ratio for the fiber and matrix are $E_f = 72,500$ MPa, $v_f = 0.22$ and $E_m = 2600$ MPa, $v_m = 0.40$, respectively. For a pure shear deformation mode we apply the following two different sets of boundary conditions to the RVE model:

(a) Periodic boundary conditions, Eqs. (8):

$$\begin{aligned}&u_{AB} - u_{EF} = 0, \quad v_{AB} - v_{EF} = 0.0018\\ &u_{AE} - u_{BF} = 0.0018, \quad v_{AE} - v_{BF} = 0\\ &u_F = v_F = 0 \quad \text{(to eliminate the rigid body motion)}\end{aligned} \tag{22}$$

where u and v are displacement components along X and Y, respectively.

(b) Homogeneous boundary conditions:

The following homogeneous boundary conditions were suggested by Aboudi (1991) to be applied to the boundary surface S of a representative volume element V:

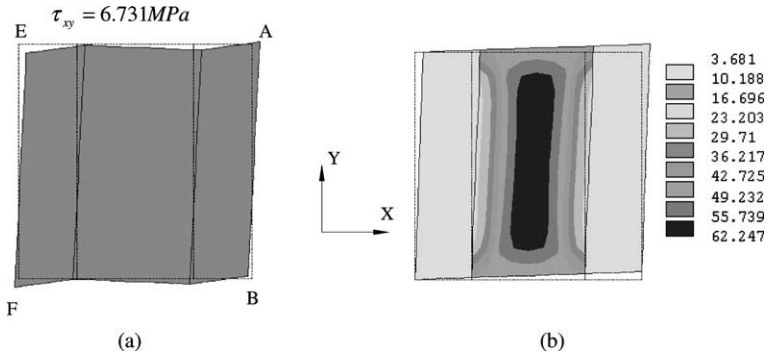

Fig. 4. Deformed shape and shear stress distribution of a two dimensional RVE model with different applied boundary conditions: (a) Eq. (22); (b) Eq. (24) (dashed lines show the undeformed shape).

$$u_i(S) = \varepsilon^0_{ij} x_j \tag{23}$$

where ε^0_{ij} is the average strain (Eq. (1.35) in Aboudi, 1991).

For the current example, the above equation reduces to

$$\begin{aligned} &u_{AB} = 0.0018 y_{AB}, \quad u_{EF} = 0.0018 y_{EF} \\ &v_{AB} = 0.0018 x_{AB} = 0.0018, \quad v_{EF} = 0.0018 x_{EF} = 0 \\ &u_{AE} = 0.0018 y_{AE} = 0.0018, \quad u_{BF} = 0.0018 y_{BF} = 0 \\ &v_{AE} = 0.0018 x_{AE}, \quad v_{BF} = 0.0018 x_{BF} \end{aligned} \tag{24}$$

Note that the origin of the coordinate system is set at the point F of the square RVE and the above boundary conditions specify that all displacement components are linearly distributed at the boundaries, i.e. a plane-remains-plane.

4.1.1. Results of finite element analysis

Case (a). The deformed shape for this case is shown in Fig. 4(a). One notes that the boundaries do not remain planes after the deformation. The resultant tractions at the boundaries are

$$\text{at AE and BF: } Nyx = \pm 6.4831,\ Nyy = 0; \quad \text{at AB and EF: } Nxx = 0,\ Nxy = \pm 6.4831$$

Further examination of the stress distribution indicates that at all boundaries the normal stress components are zero and the shear stresses are uniform in the whole body as shown in Fig. 4b, i.e. the RVE is subject to a pure shear load. In addition, not only the displacements but also the stress distributions along the boundaries satisfy the periodic conditions. Therefore, the average shear strain and the average shear stress can be calculated from Eqs. (13) and (15) resulting in $\overline{\gamma} = 2\overline{\varepsilon}_{xy} = 0.0036$ and $\overline{\tau} = \overline{\sigma}_{xy} = 6.4831$ MPa, respectively, and the equivalent shear modulus is $G = 1801$ MPa.

Case (b). The deformed shape is shown in Fig. 4(b). The boundary lines remain straight lines. Therefore, the displacement periodicity is satisfied but it is an over-constrained condition in comparison with the results in Fig. 4(a). Now let us look at the resultant forces and moments at the boundaries. They are

$$\begin{aligned} &\text{At AE and BF: } Nyx = \pm 24.335,\ Nyy = 0,\ M_1 = 10.3494 \\ &\text{At AB and EF: } Nxx = 0,\ Nxy = \pm 4.5963,\ M_2 = 0.4807 \end{aligned}$$

Note that in this case the resultant shear forces at the boundaries AE and AB are not equal. This indicates that the unit cell is not subject to a pure shear force and other forces (moments) must be applied to the boundaries in order to maintain force and moment equilibrium, see Fig. 5(a). Fig. 5(a) and (b) also show the distributions of stress components σ_x and σ_y, respectively. It is seen that the σ_x and σ_y give rise to boundary moments M_2 and M_1 to ensure that the unit cell as a whole is in equilibrium. However, the normal traction at the corresponding points on the opposite sides have opposite signs; one is in tension while the other in compression as seen in Fig. 5(b) at points C and D. This implies that the traction distribution at the corresponding opposite boundaries does not satisfy the periodic condition and as such a "RVE" model cannot be arranged in a periodic array to represent a composite material. Accordingly, it is clear that the "homogeneous displacement boundary conditions" are not appropriate boundary conditions for the RVE of composite materials subject to a shear load.

The average shear strain and the average shear stress in this case are $\overline{\gamma} = 2\varepsilon^0_{xy} = 0.0036$ and $\overline{\tau} = \overline{\sigma}_{xy} = 24.972$ MPa, respectively, and the equivalent shear modulus is $G = 6937$ MPa. We can see that the homogeneous displacement boundary condition does greatly overestimate the modulus.

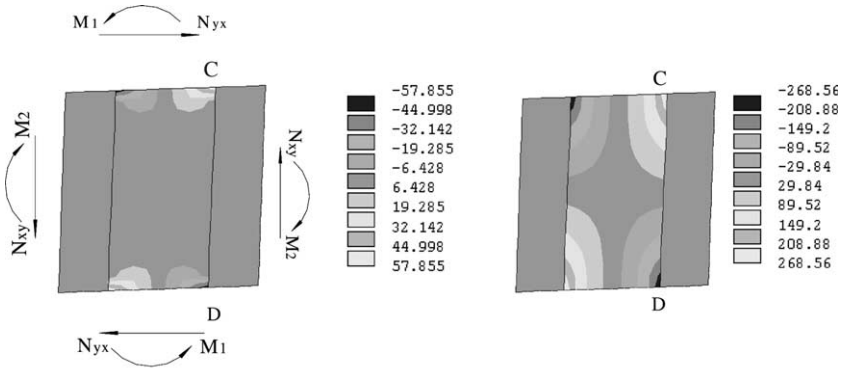

Fig. 5. Resultant boundary forces and distribution of stress components by applying homogeneous boundary conditions: (a) distribution of σ_x; (b) distribution of σ_y.

4.2. Prediction of the elastic constants of a unidirectional laminate

The unidirectional laminate is assumed to be orthotropic and linearly elastic. In a matrix notation form, the constitutive relation of this effective material can be written as

$$[\overline{\varepsilon}] = [S][\overline{\sigma}] \tag{25}$$

where $[S]$ is the compliance matrix,

$$[S] = \begin{bmatrix} S_{11} & S_{12} & S_{13} & 0 & 0 & 0 \\ S_{12} & S_{22} & S_{23} & 0 & 0 & 0 \\ S_{13} & S_{23} & S_{33} & 0 & 0 & 0 \\ 0 & 0 & 0 & S_{44} & 0 & 0 \\ 0 & 0 & 0 & 0 & S_{55} & 0 \\ 0 & 0 & 0 & 0 & 0 & S_{66} \end{bmatrix} \tag{26}$$

After obtaining the $\overline{\sigma}_{ij}$ and $\overline{\varepsilon}_{ij}$ for given c_i^j from Eqs. (13) and (15) of a RVE, the S_{ij} can be obtained from (31). The relation between the engineering elastic constants and S_{ij} are

$$\begin{aligned} E_1 &= \frac{1}{S_{11}} \quad \nu_{12} = -\frac{S_{12}}{S_{11}} \quad G_{12} = \frac{1}{2S_{44}} \\ E_2 &= \frac{1}{S_{22}} \quad \nu_{13} = -\frac{S_{13}}{S_{11}} \quad G_{13} = \frac{1}{2S_{55}} \\ E_3 &= \frac{1}{S_{33}} \quad \nu_{23} = -\frac{S_{23}}{S_{22}} \quad G_{23} = \frac{1}{2S_{66}} \end{aligned} \tag{27}$$

It should be noted that for a general orthotropic material, nine independent material constants must be determined. However, Eq. (26) contains only six equations; thus two sets of solutions are required. Note that the last three equations will result in the same moduli for the two sets of solutions. Thus, in total there are nine independent equations for nine independent material constants. All the nine constants are, therefore, determined by solving the nine equations. For a large scale problem, it is not feasible to undertake a full micromechanical simulation, instead, approaches called 'macro–micro' analysis are frequently used, whereby for a large composite structure, the micromechanical method is firstly used to predict the elastic constants of the representative points or regions of the composite structure (Moorthy and Ghosh,

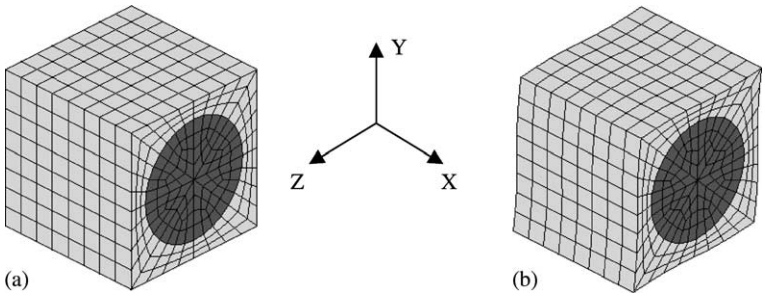

Fig. 6. (a) The finite element mesh of the RVE model for the unidirectional laminate; (b) deformed shape under shear.

1998). Thus, an efficient method of predicting elastic constants will make the macro–micro simulations more successful.

The RVE model in Fig. 1 is meshed with three-dimensional eight-node hexahedral elements. The finite element mesh is constructed with 1881 nodes and 1536 brick elements for the unidirectional RVE (Fig. 6).

The mesh grids in the opposite surfaces of the rectangular RVE are the same, i.e., the number of nodes in the opposite surfaces are equal, and the corresponding nodes on the two surfaces have the same coordinates in their plane. For example, the nodes in the plane of $x = 0$ and $x = 1$ can be related in pairs with the same y, z coordinates. This provides a considerable convenience in the implementation of the periodic boundary constraints as expressed by Eq. (8).

In this study, the unidirectional composite laminate is composed of aluminum matrix and boron fiber (model 1, shown in Fig. 1) and the angle-ply laminate is made of E-glass fiber and epoxy matrix (model 2, shown in Fig. 2). All the constituent materials are assumed to be isotropic elastic but with different material properties. Table 1 indicates the materials properties used in the calculations. The fiber volume fractions of the unidirectional lamina and angle-ply laminates are 47% and 52.5%, respectively.

The following two sets of c_i^j are used in the calculation of the unidirectional laminate model ($\Delta x = \Delta y = \Delta z = 1$):

Table 1
Material properties of fiber and matrix (Ellyin et al., 2002; Sun and Vaidya, 1996)

Material	E (MPa)	v
Boron	3.793×10^5	0.1
Aluminum	6.83×10^4	0.3
E-glass	7.25×10^4	0.22
Epoxy	2.6×10^3	0.4

Table 2
Results and comparison for unidirectional boron/aluminum laminate ($V_f = 0.47$)

Elastic constants	Present	Sun and Vaidya (1996)	Sun and Chen (1991)	Chamis (1984)	Whitney and Riley (1966)	Hashin and Rosen (1964)	Test data Kenaga et al. (1987)
E_1 (GPa)	214	215	214	214	215	215	216
E_2 (GPa)	143	144	135	156	123	135.2	140
G_{12} (GPa)	54.2	57.2	51.1	62.6	53.9	53.9	52
G_{23} (GPa)	45.7	45.9	–	43.6	–	52.3	–
v_{12}	0.195	0.19	0.19	0.20	0.19	0.195	0.29
v_{23}	0.253	0.29	–	0.31	–	0.295	–

Set 1: $c_1^1 = c_2^2 = c_3^3 = 0.012$, $c_i^j = 0.016$ $(i \neq j)$, Set 2: $c_1^1 = c_2^2 = 0.018$ all other $c_i^j = 0$.

The predicted elastic properties of the unidirectional boron/aluminum laminate ($E_3 = E_2$, $G_{13} = G_{12}$ and $v_{13} = v_{12}$) and a comparison with the numerical, analytical and the available experimental data are given in Table 2. It is to be noted that the analytical results of Hashin and Rosen (1964), based on energy variational principles, provide bounds for the elastic moduli, and the average values are used in the table.

It is seen from examining Table 2 that the predicted properties are generally in good agreement with the results in the literature, and the experimental values.

The deformed shape of the RVE under an applied pure shear periodical displacement boundary condition, $c_2^3 = c_3^2 = 0.016$, and all other $c_i^j = 0$, is shown in Fig. 6b. It is seen that the deformed boundary surfaces no longer remain planes.

4.3. Prediction of in-plane moduli for angle-ply laminates

Fig. 7 shows the meshed RVEs for $\pm 15°$ ($\pm 75°$) and $\pm 30°$ ($\pm 60°$) laminates, each having 3681 nodes and 3072 elements.

From the microstructure of the laminate, it is reasonable to assume that the laminate is orthotropic in the sense of overall response, i.e., for average stresses and average strains, we have

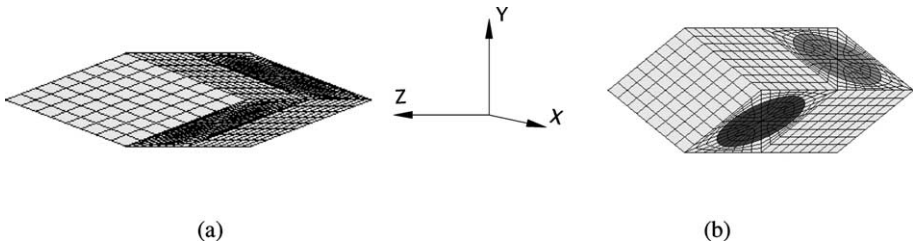

Fig. 7. Meshed RVE for angle-ply laminates (a) meshed RVE for $\pm 15°$ ($\pm 75°$); (b) meshed RVE for $\pm 30°$ ($\pm 60°$).

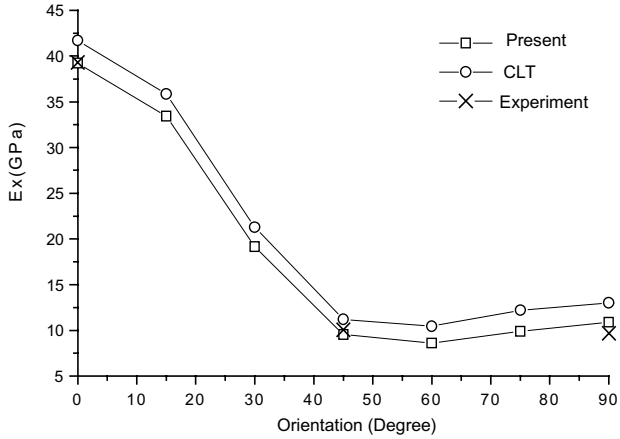

Fig. 8. E_x–θ curves for angle-ply laminates.

$$\begin{Bmatrix} \overline{\varepsilon}_x \\ \overline{\varepsilon}_y \\ \overline{\varepsilon}_{xy} \end{Bmatrix} = \begin{bmatrix} S_{11} & S_{12} & 0 \\ S_{12} & S_{22} & 0 \\ 0 & 0 & S_{66} \end{bmatrix} \begin{Bmatrix} \overline{\sigma}_x \\ \overline{\sigma}_y \\ \overline{\sigma}_{xy} \end{Bmatrix} \tag{28}$$

In a manner similar to that described in Section 4.2 above, two sets of c_1^1, c_2^2, c_1^2 are specified to obtain the elastic constants in (28). The in-plane elastic moduli can be obtained from

$$E_x = \frac{1}{S_{11}}, \quad E_y = \frac{1}{S_{22}}, \quad v_{xy} = -\frac{S_{12}}{S_{11}} \quad \text{and} \quad G_{xy} = \frac{1}{2S_{66}} \tag{29}$$

Figs. 8 and 9 show the predicted E_x and G_{xy} for angle-ply laminates with varying angles and a comparison with the results obtained by using the classical laminate theory (CLT). The lamina properties used in the CLT calculations are taken from experimental data (Hoover, 1999) and are given in Table 3.

From Figs. 8 and 9, it is seen that the differences between the results of the CLT and the present micromechanical model are rather small. And from the limited experiment points (Ellyin and Kujawski, 1995; 3M Minnesota Mining & Manufacturing Co.), it seems that the present micromechanical results are in good agreement with the experimental data. Note that the micromechanical results are based on the properties of the two constituents (fiber and matrix, Table 1), while the CLT results are based on the global properties of lamina, Table 3.

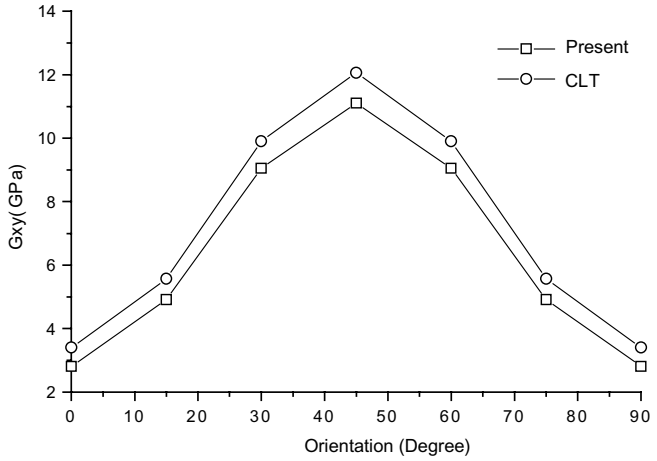

Fig. 9. G_{xy}–θ curves for angle-ply laminates.

Table 3
Elastic properties for unidirectional E-glass/epoxy lamina (Hoover, 1999)

Property	E-glass/epoxy lamina (3M-1003)
E_1 (GPa)	41.7
E_2 (GPa)	13.0
v_{12}	0.3
G_{12} (GPa)	3.4

5. Conclusions

The following conclusions are drawn from the present study:

1. An explicit unified form of boundary conditions for a parallelepiped-shaped periodic RVE model is presented which satisfy the periodicity conditions and are suitable for any combination of multiaxial loads.
2. The "homogeneous boundary conditions" (plane-remains-plane) are not only over-constrained conditions but they may also violate the stress periodicity conditions. Thus, they cannot be used to represent periodical structures of the composite laminae or laminates under loading conditions with shear components.
3. The proposed unified boundary conditions satisfy not only the boundary displacement periodicity but also boundary traction periodicity of the RVE model and as such represent periodical structures of the composite laminae or laminates under general multiaxial loading condition.
4. A meso/micro-mechanical RVE model has been developed for any angle-ply laminates.
5. A method to evaluate the average stresses and strains has been derived based on the applied boundary conditions and the resultant forces at the boundaries. By applying two sets of values of the proposed boundary conditions, all elastic moduli for the unidirectional or angle-ply laminates can be predicted simultaneously. The predicted results are in good agreement with the results available in the literature, and the experimental data.
6. The basic relations proposed in this paper do not depend on the properties of the constituent materials of a composite. Therefore, they can also be applied to nonlinear micromechanical analysis of the composites under multiaxial loads. However, all the derived equations in this paper are based on small deformation theory.

Acknowledgements

The work presented here is part of a general investigation of the mechanical properties and damage prediction of composite laminates. The research is supported, in part, by the National Science and Engineering Research Council of Canada (NSERC) through grants to Z.X. and F.E.

References

Aboudi, J., 1990. Micromechanical prediction of initial and subsequent yield surfaces of metal matrix composites. International Journal of Plasticity 6, 134–141.

Aboudi, J., 1991. Mechanics of Composite Materials, A Unified Micromechanical Approach. Elsevier Science Publishers, Amsterdam.

Adams, D.F., Crane, D.A., 1984. Finite element micromechanical analysis of a unidirectional composite including longitudinal shear loading. Computer and Structures 18, 1163–1165.

Allen, D.H., Boyd, J.G., 1993. Convergence rates for computational predictions of stiffness loss in metal matrix composites. In: Composite Materials and Structures, AMD-vol. 179/AD-vol. 37. ASME, New York, pp. 31–45.

Bakhvalov, N.S., Panasenko, G.P., 1984. Homogenization in Periodic Media, Mathematical Problems of the Mechanics of Composite Materials. Nauka, Moscow.

Benssousan, A., Lions, J.L., Papanicoulau, G., 1978. Asymptotic Analysis for Periodic Structures. North-Holland, Amsterdam.

Bigelow, C.A., 1993. Thermal residual stresses in a silicon-carbide/titanium [0/90] laminate. Journal of Composite Technology and Research 15, 304–310.

Bonora, N., Costanzi, M., Newaz, G., Marchetti, M., 1994. Micro-damage effect on the overall response of long fiber/metal matrix composites. Composites 25, 575–582.

Chamis, C.C., 1984. Simplified composite micromechanics equations for hygral, thermal and mechanical properties. SAMPE Quarterly, 14–23.

Chen, Y., Xia, Z., Ellyin, F., 2001. Evolution of residual stresses induced during curing processing using a viscoelastic micro-mechanical model. Journal of Composite Materials 35, 522–542.

Ellyin, F., Kujawski, D., 1995. Tensile and fatigue behavior of glass fiber/epoxy laminates. Construction and Building Materials 9, 425–430.

Ellyin, F., Xia, Z., Chen, Y., 2002. Viscoelastic micromechanical modeling of free edge and time effects in glass fiber/epoxy cross-ply laminates. Composites, Part A 33, 399–409.

Guedes, J.M., Kikuchi, N., 1991. Preprocessing and postprocessing for materials based on the homogenization method with adaptive finite element methods. Computer Methods in Applied Mechanics and Engineering 83, 143–198.

Hashin, Z., Shtrikman, S., 1963. A variational approach to the theory of elastic behavior of multiphase materials. Journal of Mechanics and Physics of Solids 11, 127–140.

Hashin, Z., Rosen, B.W., 1964. The elastic moduli of fiber-reinforced materials. ASME Journal of Applied Mechanics 31, 223–232.

Hollister, S.J., Kikuchi, N., 1992. A comparison of homogenization and standard mechanics analysis for periodic porous composites. Computational Mechanics 10, 73–95.

Hoover, J.W., 1999. Transverse cracking of $[\pm\theta, 90_3]_S$ composite laminates. MSc thesis, Department of Mechanical Engineering, University of Alberta, Canada.

Hori, M., Nemat-Nasser, S., 1999. On two micromechanics theories for determining micro–macro relations in heterogeneous solids. Mechanics of Materials 31, 667–682.

Kenaga, D., Doyle, J.F., Sun, C.T., 1987. The characterization of boron/aluminum in the nonlinear range as an orthotropic elastic plastic material. Journal of Composite Materials 27, 516–531.

Li, S., 1999. On the unit cell for micromechanical analysis of fiber-reinforced composites. Proceedings of the Royal Society of London, A 455, 815–838.

Moorthy, S., Ghosh, S., 1998. Particle cracking in discretely reinforced materials with the voronoi cell finite element model. International Journal of Plasticity 14, 805–827.

3M Minnesota Mining & Manufacturing Co., Technical Data of 'Scotchply' Reinforced Plastic Type 1002 & 1003. St Paul, MN, USA.

Needleman, A., Tvergaard, V., 1993. Comparison of crystal plasticity and isotropic hardening predictions for metal-matrix composites. ASME Journal of Applied Mechanics 60, 70–76.

Nemat-Nasser, S., Hori, M., 1993. Micromechanics: Overall Properties of Heterogeneous Materials. Elsevier Science Publishers, Amsterdam.

Pindera, M.J., Aboudi, J., 1998. Micromechanical analysis of yielding of metal matrix composites. International Journal of Plasticity 4, 195–214.

Raghavan, P., Moorthy, S., Ghosh, S., Pagano, N.J., 2001. Revisiting the composite laminate problem with an adaptive multi-level computational model. Composite Science and Technology 61, 1017–1040.

Sanchez-Palencia, E., 1980. Non-homogeneous Media and Vibration Theory. In: Lecture Notes in Physics, vol. 127. Springer Verlag, Berlin.

Sun, C.T., Chen, J.L., 1991. A micromechanical model for plastic behavior of fibrous composites. Composite Science and Technology 40, 115–129.

Sun, C.T., Vaidya, R.S., 1996. Prediction of composite properties from a representative volume element. Composite Science and Technology 56, 171–179.

Suquet, P., 1987. Elements of homogenization theory for inelastic solid mechanics. In: Sanchez-Palencia, E., Zaoui, A. (Eds.), Homogenization Techniques for Composite Media. Springer-Verlag, Berlin, pp. 194–275.

Whitney, J.M., Riley, M.B., 1966. Elastic properties of fiber reinforced composite materials. AIAA Journal 4, 1537–1542.

Xia, Z., Chen, Y., Ellyin, F., 2000. A meso/micro-mechanical model for damage progression in glass–fiber/epoxy cross-ply laminates by finite-element analysis. Composite Science and Technology 60, 1171–1179.